

On Improving 3D U-net Architecture

Roman Janovský^a, David Sedláček^b and Jiří Žára^c

Faculty of Electrical Engineering, Czech Technical University in Prague, Technická 2, Praha 6, Czechia

Keywords: Point Cloud, Segmentation, Neural Network, U-net, Voxel Grid.

Abstract: This paper presents a review of various techniques for improving the performance of neural networks on segmentation task using 3D convolutions and voxel grids – we provide comparison of network with and without max pooling, weighting, masking out the segmentation results, and oversampling results for imbalanced training dataset. We also present changes to 3D U-net architecture that give better results than the standard implementation. Although there are many out-performing architectures using different data input, we show, that although the voxel grids that serve as an input to the 3D U-net, have limits to what they can express, they do not reach their full potential.

1 INTRODUCTION

Convolutional neural networks are foundation for many computer vision tasks, e.g. image recognition, object classification, semantic segmentation, and other. With introduction of consumer-grade RGB-D cameras it became important to process 3D data efficiently for which 3D convolutions can be used.

In this paper we focus on the task of part segmentation, as it has many uses. However, various data representations can serve as input to the segmentation. It can be either sparse point cloud, depth images, or even mesh. This data can be augmented by additional information such as normal or colour. All these representations are missing a regular structure that could be used with convolutions, though extensive research was done to overcome this as described in Section 2. Very straightforward way is transforming the input data into a regular grid, where the 3D convolutions can be used fully exploiting the information about locality. For this task, 3D U-nets are very effective as they learn global structure and local information at the same time.

Segmentation is commonly used for labelling, where it can be useful especially in the case of augmented reality and work process. The user, given a task, has to find a part that should be maintained and segmentation could help him to find the correct part

he should focus on. This could be used as a guide for the maintainer, or as a tool to teach new hires. Segmentation can be also used as a postprocessing step for object reconstruction from images, where often unneeded parts of background can be removed. Other use cases are generation of map layers from satellite imagery such as (Hofmann and Kowshik, 2018), or in an asset creation to search for similar objects, or components for the artist to get inspired. It is also used for biomedical analysis (Milletari et al., 2016), (Çiçek et al., 2016) like tumour detection.

In the case of point cloud segmentation, many solutions exist and many of these are implemented in libraries like PCL (Rusu and Cousins, 2011). These solutions are mostly based on clustering, or cuts, which often require user input, or provide only clusters based on similarity. These clusters are usually too detailed and have to be grouped manually. Feature-based solutions can be also used, however most of the existing features for point clouds are handcrafted towards a specific task and it might not be trivial to find their optimal combination. In the case of biomedical data, the shapes can be hard to parametrize, so there was need for more expressive solution. As such, we believe the best way to be in the direction of data-oriented machine learning like neural networks. They can learn almost anything given enough annotated data (for supervised training) and can be easily extended to new objects or tasks by

^a <https://orcid.org/0000-0001-7947-867X>

^b <https://orcid.org/0000-0003-0973-0248>

^c <https://orcid.org/0000-0003-2612-7942>

training them on this new data. Thus, in the rest of the paper, we will focus on using the convolutional neural networks for segmentation. As the neural networks need to be trained, various datasets being made publicly available for such tasks, e.g. ModelNet (Wu et al., 2015), or ShapeNet (Yi et al., 2016), make the training much easier.

Though we are aware of the shortcomings of using 3D convolutions and voxel grids, e.g. feature-pose correlation as described in (Sabour et al., 2017) or the redundant operations on sparse voxels, we firmly believe that this approach can still be improved. Furthermore, as we focus on the task of model segmentation, the required input data will not suffer too much from down-sampling the data into a regular grid as would be a case of scene segmentation from RGB-D frames. In addition, regularizing the data into a grid can mitigate some noise, that can be introduced in the data. The voxel grid can also be easily constructed from mesh, point cloud, or depth image.

The structure of the paper is as follows. First, we introduce existing solutions that influenced our work in Section 2. Then we explain our network architecture and training settings in Section 3 followed by definition of a baseline, its description, and results of our experiments in Section 4.

2 PREVIOUS WORK

Neural networks work very efficiently over structured data such as 2D images, or 3D voxel grids as it can fully and easily utilize the parallelism of the GPU. As such, it leads to the use of voxel grids as they are compatible with 3D-convolutions. (Qi et al., 2016), (Wu et al., 2015), and (Maturana and Scherer, 2015) uses binary voxel grids for object classification and object segmentation. (Çiçek et al., 2016) and (Milletari et al., 2016) use 3D-convolutions for one-stage part segmentation of medical data via U-net architecture.

As voxel grids suffer from heavy memory requirements and too many unneeded multiplications by zero in empty voxels, hierarchical approaches were introduced. Kd-trees and octrees are good candidates with their regular structure as shown by Kd-networks (Klokov and Lempitsky, 2017), or O-CNN (Wang et al., 2017), and OctNet (Riegler et al., 2017) that uses hybrid grid of shallow octrees.

Neural networks proved to work well for 2D images, so multi-view CNNs (Kanezaki et al., 2018), (Qi et al., 2016), (Su et al., 2015) render 3D point cloud from multiple angles into 2D images and apply

2D-convolutions. These networks work really well for tasks as object classification, retrieval, or pose estimation. However, when the point cloud is rendered it loses information in the presence of self-occlusion. As such, these architectures are not well suited for per-point segmentation tasks.

PointNet (Qi et al., 2017) is the first network that uses unordered point cloud as its input data. It uses channel-wise max pooling to aggregate per-point features into a global feature. Furthermore, this operation is permutation invariant and with the network shared between every point, the network is invariant to the point permutation. However, the network does not include spatial information as standard convolution does. The new PointNet++ (Qi et al., 2017) groups points into a hierarchical structure. SO-Net (Li et al., 2018) imposes structure to the point cloud using self-organizing map to model the distribution of the point cloud. A position of each point in respect to the k-nearest neighbours on the map is used as an input to the network. PointNet architecture is further used in Similarity Group Proposal Network (Wang et al., 2018) which learns similarity matrix upon PointNet/PointNet++ feature vector.

Recently, architectures simulating convolutions over point patches are emerging with the state-of-the-art segmentation results. PointCNN (Li et al., 2018) reports 86.14% on ShapeNetParts. PointCNN introduces X-conv operator that first individually lifts points to higher dimension, learns transformation matrix, and then applies convolution. Similarly, effective is SpiderCNN (Xu et al., 2018) that parametrizes general convolution filter.

3 NETWORK

Although other architectures proved to yield superior results, we try to improve 3D U-net for segmentation of a point cloud as we believe that the architecture could still be improved. We propose the use of 3D voxel occupancy grid as it can be constructed simply and fast from point cloud, mesh, or depth image. Furthermore, 3D-convolution networks can be trained on a small dataset and yield good results as shown in medical applications by (Çiçek et al., 2016) or (Milletari et al., 2016). Our aim is to achieve better results by modifying such architectures, applying different techniques, and to prove it by a serious comparison of results.

3.1 Network Architecture

Our network is a 3D U-net (Çiçek et al., 2016) type of neural network with added category classification. The category prediction of the voxel grid is not required, e.g. for segmenting out objects in a room, or for segmentation of medical data. Thus, the 3D U-net in itself does not require prior knowledge about the category of the input. However, during the training, when using this prior knowledge as an addition to the loss function, the network does yield better results.

The network is composed of two parts: classification (down-sampling) and segmentation (up-sampling) as depicted in Figure 2. Each part consists of three blocks.

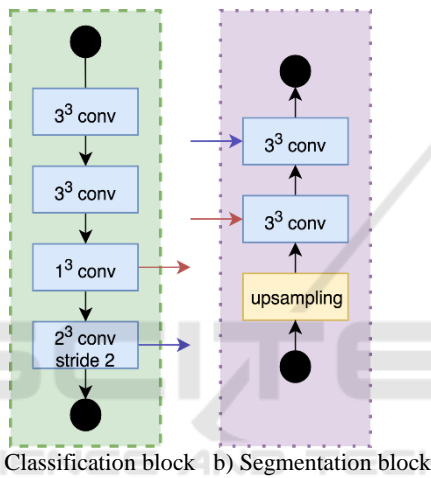


Figure 1: Basic building blocks of a) classification on the left, and b) segmentation layer on the right.

The main building block of the classification part of our network is shown in Figure 1 a). We apply two 3D convolutions with zero padding to keep the dimensions of the input, which are followed by batch normalization. The results are then concatenated, and convolution of size 2^3 with stride 2 is applied to half the resolution of the input grid.

After each convolution, we use batch normalization (Ioffe and Szegedy, 2015) and dropout (Srivastava et al., 2014). ReLU (Nair and Hinton, 2010) activation function is used for the classification part, and softplus (Zhao et al., 2018) for the segmentation (except for the last prediction layers).

After the third classification block, we use maxout (Goodfellow et al., 2013) to convert the grid into a one-dimensional vector of size 512, which is fed into the classification multilayer perceptron (MLP) and softmax layer. We also use the feature vector to estimate mask for all possible object parts.

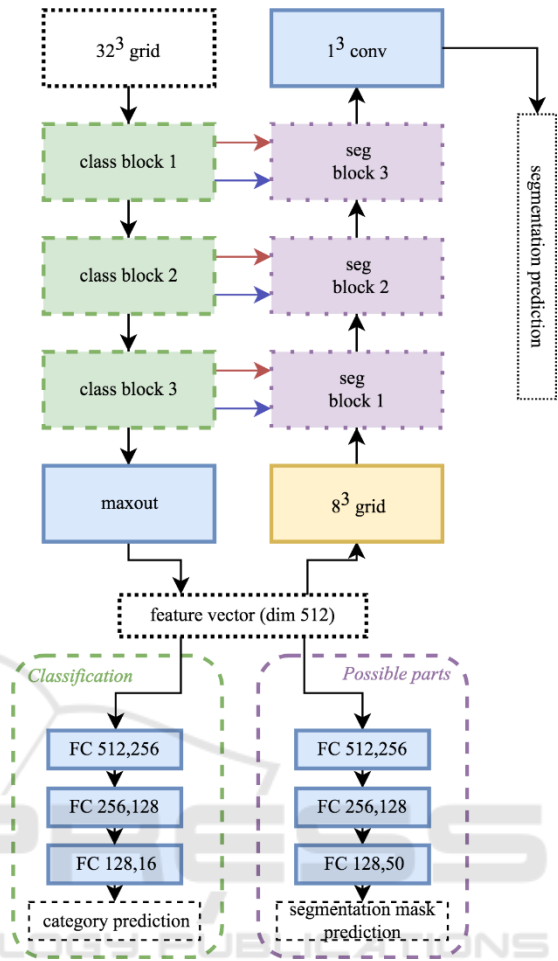


Figure 2: Architecture of our U-net neural network with category prediction and segmentation.

The feature vector is tiled into a grid of size 8^3 which is the input into the segmentation part. The segmentation part of the network uses blocks as depicted in Figure 1 b). The first convolution of segmentation block down-samples the number of channels to the half of the input voxel grid, i.e. with the input number of channels C_i , and C_s channels from skip connection we have C_i+C_s filters of size $C_i/2$. The following segmentation block uses the up-sampled grid from previous block. If not said otherwise, we also zero-pad the input grid to keep its dimensions.

As there will always be a loss of information when up-/down-sampling, we try to compensate this by using skip connections. We add output of the strided convolutions right before up-sampling and output of 1^3 convolution right after up-sampling.

3.2 Implementation Details

Our network is implemented using TensorFlow (Abadi et al., 2015). We use Adam optimization (Kingma and Ba, 2014) to minimize sum of softmax cross entropies – sum over segmentation, sum over possible mask, and sum over category. We also multiply the input segmentation by the occupancy grid, so that the network focuses on minimizing valid voxels. We use the Adam optimization with an initial learning rate of 0.0001 and batch size of 16. We decrease the learning rate by 0.75 each five epochs. The network generally converges around the 10th epoch with batch normalization. We also apply gradient clipping in range $<-1,1>$. Each layer is followed by dropout layer with keep probability 75%.

4 EXPERIMENTS

The performance of our network has been evaluated on two different applications – **object classification** and **part segmentation**. In this chapter, we describe data used, our baseline network, changes to the architecture, and report how they affect the training and network generalization.

4.1 Metrics

For comparison of **part segmentation** results we use weighted average Intersection over Union (IoU) as provided by (Yi et al., 2016). Per category average IoU is computed for each category first by averaging across all parts of all shapes with the certain category label. The overall average IoU is then computed through a weighted average of a per-category IoU. The weights are the number of samples in each category. To compare ourselves on **object classification** task we use per instance accuracy on ModelNet (Wu et al., 2015).

4.2 Datasets

For **object classification** we use two variants of ModelNet (Wu et al., 2015), i.e. ModelNet40 and its subset ModelNet10. The ModelNet40 contains 13,834 objects from 40 different categories, where 9,834 are used as training samples and 3,991 as the test samples. ModelNet10 has 2,468 training samples and 909 test samples. Since the original ModelNet contains models represented by edges and vertices, we use pre-generated dataset of point clouds from authors of PointNet++ (Qi et al., 2017), where each model is uniformly sampled by 10,000 points.

For the **part segmentation** task, we use ShapeNetPart dataset (Yi et al., 2016). It contains 16,881 objects in 16 categories, represented as point clouds. Each object consists of 2 to 6 parts with 50 parts in total, where an object does not need to have all category parts. We use the formal split, where dataset is split into 12,137 objects for the train set, 1,870 objects for the validation set, and 2,874 objects for the test set.

4.3 Baseline Network

We based our network on the standard 3D U-net architecture. The baseline network has similar structure to network depicted in Figure 2. However, each block consists of two 3^3 convolution layers followed by max pooling instead of 2^3 convolutions with stride 2. The baseline also uses convolution 4^3 instead of maxout. The filter output size is (32,64,128) for the classification blocks and (256,128,64) for the segmentation blocks. The baseline network has ~13.3M trainable parameters and uses only ReLU as activation function.

With the baseline and no modifications to the dataset we were able to reach 78.8% IoU. However, the training suffered from category imbalance (Figure 4) because the network tends to overfit on categories with higher number of samples. We discuss the problem in the following sections.

4.4 Removing Max Pooling

As max pooling can lead to the loss of information, we tried to replace max-pooling layers with convolution layers of size 2^3 and stride 2. They halve the resolution and double the number of channels. This made the training more stable, but increased the number of trainable parameters to ~19.5M, where most of it was contributed by the 4^3 convolution, that was used instead of the maxout layer in Figure 2. Replacing the max pooling raised the IoU to 80.5%.

Though this increased the overall performance, the network still fails at small parts as thin straps, or very low-detailed transitions such as gas tank/saddle and motorbike body, or transition between the tip and the rest of the rocket. Ground truth for these categories is shown in Figure 3.

4.5 Category Imbalance

As shown in Figure 4, the ShapeNetPart dataset suffers from category unbalance, where in the train set *table* category has 100 times more samples than the *cap* category. As such, the network is likely to

learn more on these large categories, because the accumulated loss will be higher for the large categories. The same goes for the test set, where the categories *table*, *chair*, and *airplane* contribute to the result by 65%. Figure 5 shows how can large categories influence the weighted IoU in comparison to the average.

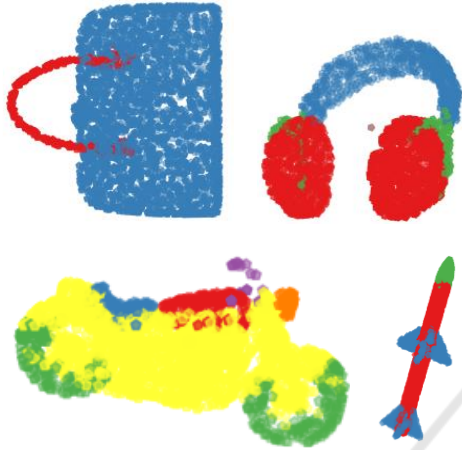


Figure 3: Ground truth for problematic categories - bag, earphones, rocket, and motorbike. Especially, the red strap for the bag (top left), green straps for the earphones (top right), green tip of a rocket (bottom right), and motorbike parts except the yellow body (bottom left) are often misclassified as neighbouring parts.

We considered simple weighting based on the distribution of the data, but given the fact that for large categories the value is close to zero and for small categories it is evenly distributed, it did not significantly change the training. As the simple weighting did not help, we tried to apply probabilistic weights, which is discussed in the following section.

4.6 Probabilistic Weights

Softmax function takes the input vector and normalizes the sum of the vector to 1 where each element is in range $\langle 0,1 \rangle$. Given these properties, it can also be interpreted as a probabilistic distribution saying how likely is each part.

We use these probabilities to weight the output of the softmax cross entropy loss function by $(2-P)$, where P is the estimated probability of the correct label. This way the voxels with lower probability have higher impact on the training. Even though it improved the overall IoU, it did not solve the problem with category imbalance.

Weighting also proved to have a regularization effect, lowering the variance between test and train

data. When weighting was not used the cost and accuracy on the train set would decrease and increase respectively, but the accuracy on the test data was decreasing as the network started to overfit. With the weighting applied the network tries not to favour any voxel and thus slowing the overfitting process. In respect to the backpropagation the weighting works as additional max term for the correct label whereas

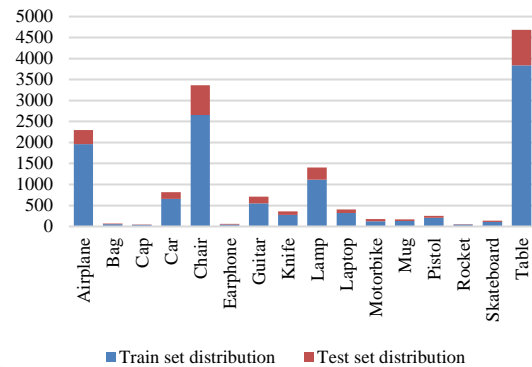


Figure 4: Number of samples per category. ShapeNetPart training (blue) and test (red) data sample distribution among the 16 categories.

the loss itself maximizes the difference between correct label and the others.

Though the network learned better on the hard categories like cap, rocket, or motorbike, it did not improve the weighted average IoU.

4.7 Oversampling

When using random permutation of the dataset for each training epoch, the final result depends on the luck of the draw, i.e. when the small categories are not in one of the last batches, their IoU drastically drops. This can be seen in Figure 6, where the blue line shows weighted average IoU with value of 82%. However, the categories with high number of samples contribute to the overall IoU the most, and as such there is a significant drop in harder categories like cap, motorbike, or rocket.

To prevent this behaviour, we oversample the training set so that each category contains the same number of samples as the largest category, and each batch has exactly one sample from each category.

We trained the network again but with oversampling. For comparison, we took this newly trained model and compared it with a network trained without oversampling, but having similar IoU.

The results comparing training with/without the oversampling are shown in Figure 6, red without oversampling and green with oversampling. Both

these networks do clearly overfit less, however with oversampling, the network outperforms on the hard categories (cap, earphone, motorbike, rocket).

Oversampling increases the training time and prevents the overfitting, but lowers the overall accuracy reaching 80.9% IoU. As it repeats some samples multiple times, we tried simple data augmentation, i.e. rotation and scale of the point cloud.

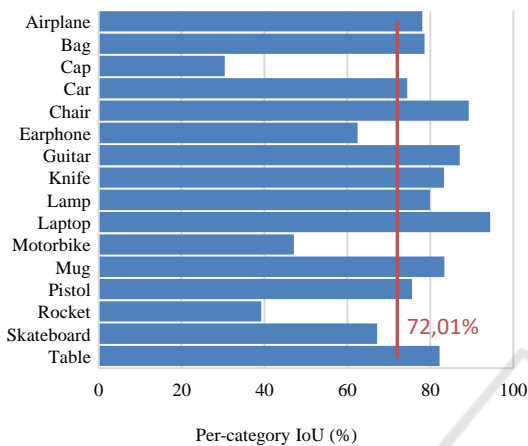


Figure 5: The influence of largest categories on weighted IoU. Case when the three largest categories in test set, as can be seen in Figure 4 (table, airplane, chair), keeps the weighted IoU on 82% even though the average is lower – 72% marked in graph by red solid line.

When compared with weighting, data augmentation had better regularization effect, and got the IoU at maximum of 82.2%, whereas with the weighting it reached its maximum at 80.8%.

4.8 Segmentation Mask

Convolutional neural networks are good at finding the overall structure of the input data, but do not handle well correct placement of each respective parts often thanks to the max pooling, i.e. it does not matter where the eye in the face is as long as it is there.

We tried to leverage the category classification capabilities by converting the predicted category into a mask to remove category misclassifications as the network can reach 97.5% category prediction accuracy on the test data.

We tried two different approaches: a) learn the mask during training, and b) generate the mask from predicted category.

As for a) learning the mask, we tried to learn two different masks – all possible parts for category and all possible parts for given sample; does not need to have all category parts like standing/hanging lamp.

Both approaches led to similar results, however learning mask for given sample yields slightly better results.

Approach b) gave cleaner results, but category misclassifications became more apparent. However, when the category is misclassified most of the voxels are misclassified as well. Moreover, most of the parts are misclassified in its own category, except categories like cap, rocket, earphone, and lamp,

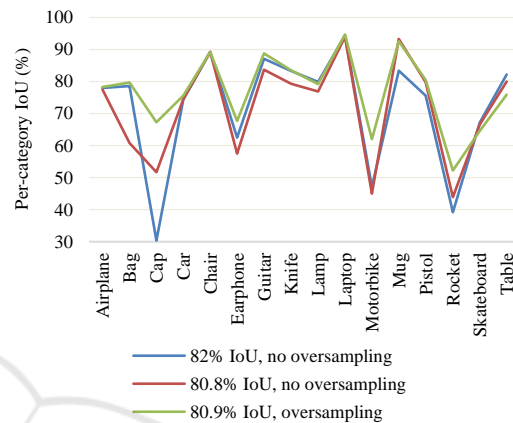


Figure 6: Comparison of evaluation on the test set, when trained with and without oversampling. For this comparison, learned models with similar wIoU are used. The network model used is the variant of baseline architecture with convolutions instead of max pooling.

where significant number of voxel misclassifications is in different category. As such, masking out the segmentation results as postprocess seems like a valid strategy that does not introduce too much inaccuracies when applied on not-fully trained network.

Though the IoU was not improved, when we compared confusion matrices, the misclassifications were more focused in the categories themselves.

4.9 Segmentation Results

As the network has large number of trainable parameters, where most of them are from the last down-sampling layers, we replaced the last 4³ convolution with maxout (Goodfellow et al., 2013) lowering the number of trainable parameters to ~11.1M without affecting the performance.

The network can be trained in 16 hours with inference time of 20ms per sample. We use augmentation, oversampling, and learn the segmentation mask, though we don't apply the mask. We also tried various activation functions for the

Table 1: Object part segmentation results on ShapeNetPart dataset.

Method	Intersection over Union (IoU)																
	Mean	air.	bag	cap	car	chair	ear.	gui.	knife	lamp	lap.	motor	mug	pistol	rocket	skate	table
Kd-Net	82.3	80.1	74.6	74.3	70.3	88.6	73.5	90.2	87.2	81.0	94.9	57.4	86.7	78.1	51.8	69.9	80.3
PointNet	83.7	83.4	78.7	82.5	74.9	89.6	73.0	91.5	85.9	80.8	95.3	65.2	93.0	81.2	57.9	72.8	80.6
SO-Net	84.9	82.8	77.8	88.0	77.3	90.6	73.5	90.7	83.9	82.8	94.8	69.1	94.2	80.9	53.1	72.9	83.0
PointNet++	85.1	82.4	79.0	87.7	77.3	90.8	71.8	91.0	85.9	83.7	95.3	71.6	94.1	81.3	58.7	76.4	82.6
SpiderCNN	85.3	83.5	81.0	87.2	77.5	90.7	76.8	91.1	87.3	83.3	95.8	70.2	93.5	82.7	59.7	75.8	82.8
SGPN	85.8	80.4	78.6	78.8	71.5	88.6	78.0	90.9	83.0	78.8	95.8	77.8	93.8	87.4	60.1	92.3	89.4
O-CNN+CRF	85.9	85.5	87.1	84.7	77.0	91.1	85.1	91.9	87.4	83.3	95.4	56.9	96.2	81.6	83.5	74.1	84.4
PointCNN	86.1	84.1	86.5	86.0	80.8	90.6	79.7	92.3	88.4	85.3	96.1	77.2	95.3	84.2	64.2	80.0	83.0
Ours	82.2	77.7	84.4	84.2	76.6	88.7	76.0	88.1	82.3	81.4	94.6	68.0	95.1	81.5	52.5	70.9	78.7

segmentation part with softplus function (Zhao et al., 2018) yielding best results.

We present our results in Table 1, where we compare our results with the state-of-the-art methods for object part segmentation. It can be seen that our network falls behind most of the architectures. Our network suffers from having not enough local information. However, simply increasing the resolution of the input voxel grid doesn't improve the results: doubling the resolution slightly lowered the accuracy. To improve the local information, we tried to change the input to a vector per voxel, where the vector is composed from directions from the voxel mean to k-nearest points. Though not yielding notable results, the voxel grid could serve as a look-up table for other methods struggling with global structure encoding.

4.10 Classification Results

The network used for tests on ModelNet10 and ModelNet40 was the same network as depicted in Figure 2 although we stripped the network of all parts that are required for segmentation. Resulting network has ~2.2M trainable parameters. With oversampling and augmentation, the training time per sample is 25ms and inference time is 3ms. We trained the network on ModelNet10/40 with batch size of 40. The network can be trained in 12 hours on ModelNet40.

As shown in Table 2, we compare ourselves with other approaches also used for segmentation. Moreover, we include 3DShapeNets (Wu et al., 2015) since they use a voxel grid as an input and RotationNet (Kanazaki et al., 2018) as the best reported result on Princeton ModelNet.

To the best of our knowledge, we outperform or match most of the existing solutions for object classification using voxel grids, although each network was fine-tuned on different type of application. However, in comparison with architectures working on other data structures our approach does not reach notable results.

Table 2: Object classification results on ModelNet10 and ModelNet40 for methods using point cloud, voxel grid, Kd-tree, octree, or self-organizing map as an input. Networks using voxel grids are listed under the dashed line.

Method	ModelNet40 Classification Accuracy	ModelNet10 Classification Accuracy
PointNet	89.2	-
PointNet++	91.9	-
Kd-Net	91.8	94.0
O-CNN	90.6	-
SO-Net	93.4	95.7
SpiderCNN	92.4	-
PointCNN	84.5	91.0
RotationNet	97.3	98.5
3DShapeNets	77.0	83.5
binVoxNetPlus	85.5	92.3
VoxNet	83	92
ORION	-	93.8
Ours	88.8	93.0

5 CONCLUSION

In this paper, we had presented modifications to 3D U-net architecture and in the series of experiments shown their influence on the training process and ability to generalise. We show improvements from the baseline architecture by 3% on the segmentation task. As voxel grids provide hierarchical global information, we see a promising way to further improve the voxel-based architectures by combining it with approaches focused more on local features, or with refinement methods.

ACKNOWLEDGEMENTS

This work is supported by Ministry of Education, Youth and Sports within the project Key technologies for Time-Of-Flight sensor data processing and

visualization (LTACH17013). The authors acknowledge the support of the OP VVV MEYS funded project CZ.02.1.01/0.0/0.0/16_019/0000765 „Research Center for Informatics“.

REFERENCES

- Abadi, M. et al., 2015. *TensorFlow: Large-Scale Machine Learning on Heterogeneous Systems*.
- Çiçek, Ö. et al., 2016. 3D U-Net: learning dense volumetric segmentation from sparse annotation. In *Medical Image Computing and Computer-Assisted Intervention – MICCAI 2016*., pp.424-432.
- Goodfellow, IJ. et al., 2013. Maxout Networks. In *Proceedings of The 30th International Conference on Machine Learning*.
- Hofmann, D. and Kowshik, B., 2018. *Meet RoboSat - End-to-end feature extraction from aerial and satellite imagery*. [online] Available at: <https://blog.mapbox.com/meet-robosat-af42530f163f> [Accessed 25 Feb. 2019].
- Ioffe, S. and Szegedy, C., 2015. Batch Normalization: Accelerating Deep Network Training by Reducing Internal Covariate Shift. *International Conference on Machine Learning*., pp.448-456.
- Kanezaki, A., Matsushita, Y. and Nishida, Y., 2018. RotationNet: Joint Object Categorization and Pose Estimation Using Multiviews from Unsupervised Viewpoints. In *2018 IEEE/CVF Conference on Computer Vision and Pattern Recognition*., pp.5010-5019.
- Kingma, D. P. and Ba, J., 2014. Adam: A method for stochastic optimization. *arXiv preprint arXiv:1412.6980*.
- Klokov, R. and Lempitsky, VS., 2017. Escape from Cells: Deep Kd-Networks for the Recognition of 3D Point Cloud Models. In *2017 IEEE International Conference on Computer Vision (ICCV)*., pp.863-872.
- Li, Y. et al., 2018. PointCNN: Convolution On X-Transformed Points. In *Advances in Neural Information Processing Systems*., pp.828-838.
- Li, J., Chen, BM. and Lee, GH., 2018. SO-Net: Self-Organizing Network for Point Cloud Analysis. In *2018 IEEE/CVF Conference on Computer Vision and Pattern Recognition*., pp.9397-9406.
- Maturana, D. and Scherer, S., 2015. VoxNet: A 3D Convolutional Neural Network for real-time object recognition. In *2015 IEEE/RSJ International Conference on Intelligent Robots and Systems (IROS)*., pp.922-928.
- Milletari, F., Navab, N. and Ahmadi, SA., 2016. V-Net: Fully Convolutional Neural Networks for Volumetric Medical Image Segmentation. In *2016 Fourth International Conference on 3D Vision (3DV)*., pp.565-571.
- Nair, V. and Hinton, GE., 2010. Rectified Linear Units Improve Restricted Boltzmann Machines. In *Proceedings of the 27th International Conference on Machine Learning*., pp.807-814.
- Qi, C. R. et al., 2017. PointNet: Deep Learning on Point Sets for 3D Classification and Segmentation. In *2017 IEEE Conference on Computer Vision and Pattern Recognition (CVPR)*., pp.77-85.
- Qi, C. R. et al., 2016. Volumetric and Multi-view CNNs for Object Classification on 3D Data. In *2016 IEEE Conference on Computer Vision and Pattern Recognition (CVPR)*., pp.5648-5656.
- Qi, C. R. et al., 2017. Pointnet++: Deep hierarchical feature learning on point sets in a metric space. In *Advances in Neural Information Processing Systems*., pp.5099-5108.
- Riegler, G., Ulusoy, AO. and Geiger, A., 2017. OctNet: Learning Deep 3D Representations at High Resolutions. In *2017 IEEE Conference on Computer Vision and Pattern Recognition (CVPR)*., pp.6620-6629.
- Rusu, RB. and Cousins, S., 2011. 3D is here: Point Cloud Library (PCL). In *2011 IEEE International Conference on Robotics and Automation*., pp.1-4.
- Sabour, S., Frosst, N. and Hinton, GE., 2017. Dynamic Routing Between Capsules. *Neural Information Processing Systems*., pp.3856-3866.
- Srivastava, N. et al., 2014. Dropout: a simple way to prevent neural networks from overfitting. *Journal of Machine Learning Research*. **15**(1), pp.1929-1958.
- Su, H. et al., 2015. Multi-view convolutional neural networks for 3d shape recognition. In *Proc. ICCV*.
- Wang, PS. et al., 2017. O-cnn: Octree-based convolutional neural networks for 3d shape analysis. *ACM Transactions on Graphics (TOG)*. **36**, p.72.
- Wang, W. et al., 2018. SGPN: Similarity Group Proposal Network for 3D Point Cloud Instance Segmentation. In *2018 IEEE/CVF Conference on Computer Vision and Pattern Recognition*., pp.2569-2578.
- Wu, Z. et al., 2015. 3D ShapeNets: A deep representation for volumetric shapes. In *2015 IEEE Conference on Computer Vision and Pattern Recognition (CVPR)*., pp.1912-1920.
- Xu, Y. et al., 2018. SpiderCNN: Deep Learning on Point Sets with Parameterized Convolutional Filters. *European conference on computer vision*., pp.90-105.
- Yi, L. et al., 2016. A Scalable Active Framework for Region Annotation in 3D Shape Collections. *SIGGRAPH Asia*.
- Zhao, H. et al., 2018. A novel softplus linear unit for deep convolutional neural networks. *Applied Intelligence*. **48**(7), pp.1707-1720.